DEUTSCHES ELEKTRONEN-SYNCHROTRON DESY

DESY SR-81/01
February 1981

3 d-VALENCE ORBITAL STRUCTURE OF Zn-PHTHALOCYANINE; RESULTS FROM PHOTOEMISSION EXPERIMENTS AND CLUSTER CALCULATIONS

by

E. E. Koch
Hamburger Synchrotronstrahlungslabor HASYLAB
at
Deutsches Elektronen-Synchrotron DESY, Hamburg

M. Iwan
II. Institut für Experimentalphysik der Universität Hamburg

K. Hermann
Institut für Theoretische Physik B, TU Clausthal

P. S. Bagus
IBM San José Research Laboratory, San José, California 95193, USA

NOTKESTRASSE 85 · 2 HAMBURG 52

DESY SR-81/01
February 1981

3 d-Valence Orbital Structure of Zn-Phthalocyanine; Results from Photoemission Experiments and Cluster Calculations

E. E. Koch

Hamburger Synchrotronstrahlungslabor HASYLAB, Deutsches Elektronen-Synchrotron DESY, 2000 Hamburg 52, Germany

M. Iwan*

II. Institut für Experimentalphysik der Universität Hamburg, 2000 Hamburg 50, Germany

K. Hermann

Institut für Theoretische Physik B, TU Clausthal, 3392 Clausthal-Zellerfeld, Germany, and Sonderforschungsbereich 126 Clausthal/Göttingen

and

P. S. Bagus**

IBM San José Research Laboratory, San José, California 95193, USA

---

* now at Fritz-Haber-Institut, 1000 Berlin 33

** Alexander von Humboldt awardee 1979/1980

- submitted to Chem. Phys. -

Abstract

We have determined the binding energies (initial energies) for the Zn 3d-derived density of states in Zn-Phthalocyanine (ZnPC) from photoelectron energy distribution curves obtained with photon energies ranging from 30 eV to 120 eV by exploiting the strong hν - dependence of the 3d partial cross-section. The center of the 3d derived states is located 15.2 eV below the vacuum level ($E_{VAC} = 0$) and is 1.2 eV wide (FWHM). The experimental results are compared with ab initio Hartree-Fock-LCAO calculations on ZnN_4 clusters. The fully relaxed ionization potentials (IP) derived from self-consistent wavefunctions of the different d-hole states of ZnN_4 are smaller by about 6eV with respect to the Koopmans IP's. This relaxation shift brings the calculated center of the 3d derived states in close agreement with experiment. The relative positions of the calculated 3d-type levels in ZnN_4 are also consistent with a simple ligand field model of the ZnPC complex where reasonable interaction parameters are used.

I. Introduction

The electronic structure of the valence bands of metal free and metal-phthalocyanines (PC's) has recently been the subject of many theoretical (see e.g. Ref. 1 - 3) and experimental studies (see e.g. Ref. 4 - 11). In particular, recent photoelectron energy distribution (EDC) measurements on PC's have shown a fairly complex structure of the valence bands extending over a binding energy range from 5 eV to 35 eV (7 - 11). In view of the many overlapping orbitals it is in general not easy to disentangle the complicated partial density of states. The binding energies, possible splittings and relative strengths of the metal derived orbitals are of particular interest and efforts have been made in the past to tackle this problem experimentally (see Ref. 5 - 11).

In the present paper we report on a combined experimental and theoretical effort in order to elucidate the 3d-valence orbital structure of Zn-Phthalocyanine. For Zn the atomic ground state configuration is $3d^{10}4s^2$ and the atomic photoelectron spectra show the d-states well separated from the s-states (12). This is carried through to the metallic state, where the Zn d-bands are well separated from the s-p like bands (13). Thus, ZnPC appears to be a suitable material to study the 3d-valence orbital structure and the influence of the molecular environment on the metal d-states.

By utilizing the characteristically different hν -dependencies of p-state and d-state photoelectron cross-sections in the 30 to 120 eV photon energy range, we have determined the d-partial densities of states which we then compare to results for atomic and metallic Zn. Furthermore, in order to study the influence on the transition metal atom caused by the molecular environment in ZnPC, we have performed molecular calculations on a simple model cluster. Since there is experimental evidence that the Zn-PC bonding is not too strong (14), it is reasonable to assume that the nearest neighbor environment of the metal atom accounts for most of the Zn-PC bonding interaction. Thus we include in our model cluster in addition to the central Zn atom only its four nearest nitrogen atoms resulting in a planar ZnN_4 cluster with D_{4h} symmetry (see insert in Fig. 1). For the Zn-N distance of the cluster, the experimental value from ZnPC, $d_{Zn-N} = 1.99$ Å has been used (15). Clearly, an improved model of the electronic structure of the metal atom in ZnPC would have to account also for the molecular part further away from the metal atom by some kind of perturbational treatment. However, in the present study we restrict ourselves to the simple model of an isolated ZnN_4 cluster.

2. Experimental Procedure and Results

The experiments were carried out with a commercial double-pass cylindrical mirror analyzer. Synchrotron radiation from the 240 MeV storage ring TANTALUS I at the University of Wisconsin in Madison monochromatized by a 1.5 m toroidal grating monochromator (TGM) served as a tunable light source (16). Typical count rates were 1×10^4 sec^{-1}. In general, an overall resolution of 0.3 to 0.5 eV was sufficient for the fairly broad structures in the EDCs. The experiments were carried out on thin polycrystalline films prepared from outgassed high purity powder by in situ sublimation onto a stainless steel sample holder. The preparation of the samples and the measurements have been performed under ultra-high vacuum conditions. The base pressure was 8×10^{-11} torr.

A selection of EDC's for Zn-Pc in the range of photon energies between 40 and 120 eV is displayed in Fig. 1. The binding energy scale is referred to the vacuum level $E_{VAC}=0$. The spectra have been roughly normalized by taking into account the efficiency of the TGM monochromator for different photon energies. Most of the features are due to C-, N- and H-derived π-, 2p and 2s-like molecular orbitals which span a range of initial energies from -4 eV to roughly -30 eV (11). With increasing hν, we observe a gradual increase (relative with respect to the other valence band features) of a sharp feature at an intitial energy of - 15.2 eV. This peak in the EDC's which of course is partly overlapping with other valence band states is identified as the Zn derived 3d valence orbitals. The gradual increase of the 3d cross-section is in accord with the general trend for the atomic 3d cross-sections, e.g. the calculated atomic $3d^{10}$-Kr cross-section (17) or the partial cross-section for Ga 3d (18). Photoemission measurements as shown in Fig. 1 permit relative partial cross-sections to be easily measured (e.g. Ref.7). The determination of absolute partial cross-sections has to take into account additionally a number of experimental parameters, such as the variation of the transmission of the electron energy analyzer and the hν-dependent variation of the detected volume (see e.g. Ref. 19). In the case at hand, we restrict ourselves to a qualitative analysis of the data and use the cross-section dependence merely as a diagnostic tool.

A quantitative measure of the extent of the Zn 3d contribution to the density of valence states is obtained by taking the difference spectrum between Zn-PC and H_2-PC. For $h\nu$ = 100 eV this difference spectrum is shown in Fig. 2. In Fig. 2 we also compare this difference curve with the atomic photoelectron spectrum for Zn (12) and with the EDC for Zn metal (13) in the range of the d-bands. The width of the Zn 3d derived states is only 1.2 eV ± 0.1 eV wide (FWHM). All relevant energies are collected in Table 1 and will be discussed below.

We note in passing that EDC's obtained with photon energies near the 3p threshold ($h\nu \approx 95$ eV) for Zn metal and Zn-PC show pronounced resonance satellite structures at about 20 eV below the Zn 3d main peak. These resonant-two-hole bound states have been analyzed as excitations of a quasi-bound state (shake-up multiplet) of mainly $3p \rightarrow 4s$ character followed by a decay of the 3p hole leading to a $3d^8 4s$ two-hole final state (10). These states occur at initial energies outside the range considered here and are in Zn and ZnPC well separated from the one-electron excitations. Their origin and the implications for the electronic structure of Zn-PC have been discussed in Ref. 10.

3. Model Calculations

For the calculations we restrict ourselves, as mentioned above, to the simple model of an isolated ZnN_4 cluster. Self-consistent field (SCF) analytic basis set Hartree-Fock calculations for various electronic configurations of the cluster are carried out following the Roothaan approach. The contracted Gaussian basis set for N was taken from Van Duijneveldt's calculations (20) on the free atom where 9s and 5p functions were contracted to (4, 3). The basis set for Zn was taken from Wachter's calculations (21) on the atom to which two p functions (exponents $\alpha = 0.16856$, $\alpha = 0.06276$) were added to allow for p hybridization of the Zn 4s orbital. Here 14s, 11p, 5d functions were contracted to (8, 6, 3). On the whole, the basis sets used in the present study are of better than double zeta quality and it is very unlikely that the results obtained will change significantly, if larger basis sets are used.

From calculations on various electronic configurations of the ZnN_4 cluster it was found that the lowest energy configuration is $^1A_1$ with orbital structure $7a_{1g}^2\ 3b_{1g}^2\ 1b_{2g}^2\ 2e_g^4\ 3a_{2u}^2\ 1b_{1u}^2\ \ 5e_u^4$ and a total energy of - 1994.54334 H. In this configuration the cluster is stable by 5.46 eV with respect to its atomic constituents. The ZnN_4 bonding in the model contains both ionic and covalent contributions as can be seen from a detailed Mulliken population analysis of the ground state. The gross atomic population of the Zn part shows a $3d^{9.85}4s^{0.55}4p^{0.87}$ configuration in ZnN_4 which has to be compared to the free atom configuration $3d^{10.0}4s^{2.0}4p^{0.0}$. Obviously, the ZnN_4 bonding results in a decrease of the Zn 4s occupation by about 1.5 electrons whereas the Zn 4p level, unoccupied in the free atom, contains roughly 0.9 electrons in ZnN_4. The latter result can be interpreted as some kind of partial backdonation in the cluster. On the whole, the Zn atom becomes slightly positive (by 0.7 electrons) in ZnN_4. The covalent part of the ZnN_4 bonding is characterized by the $7a_{1g}$ orbital being a mixture of N 2sp and small Zn 4s-type contributions and the 5 e_u orbital being a mixture of Zn 4p and N 2p type functions which accounts mainly for the 4p back-donation mentioned above. In addition, the 2 b_{1g} orbital indicates quite small Zn $3d_{xy}$ - N 2s coupling. Contour plots of the relevant orbitals are shown in Fig. 3.

In Figure 4 the Hartree-Fock one-electron energies ϵ of the ZnN_4 valence orbitals are shown. Obviously, the energy levels can be grouped into three regions that are well separated. Region I between 27.5 and 29.5 eV refers to orbitals that are characterized mainly by N 2s-type contributions with quite small Zn 3d admixtures. The levels of region II between 22.0 and 24.5 eV belong to orbitals of Zn 3d character with small N 2sp admixtures and those of region III between 11.5 and 14.0 eV are due to orbitals that are mostly N 2p-type with minor Zn 4s and 4p type contributions. Therefore, in a photoemission measurement on the planar ZnN_4 cluster one should be able to distinguish clearly between 3d emission from the central Zn atom and valence emission from the surrounding N_4 complex. For a comparison with photoemission data on ZnPC the calculated ZnN_4 valence level structure has to be modified, because of the presence of the peripheral PC part around the ZnN_4 cluster in ZnPC. First, additional energy levels due to orbitals describing the valence electron structure of the peripheral PC part must arise and can spread over the whole energy range covered in

Figure 4. Second, the ZnN_4 energy levels of region I and III, referring to orbitals that are mainly concentrated on the N centers of the cluster, will be shifted somewhat as these orbitals are affected by the bonding between the ZnN_4 and the peripheral PC part in ZnPC. Generally, the bonding effect will shift the respective orbital energies towards lower values. However, from the energy separations in ZnN_4 one would expect the levels of region III to be well above the Zn 3d levels (region II) even in a calculation on ZnPC. The level structure of the Zn 3d-type orbitals (region II) even in ZnN_4 will be only slightly modified by the presence of the peripheral PC part in the real system, since these orbitals are strongly localized on the central Zn atom. Therefore, the present ZnN_4 model cluster seems to be appropriate to describe the main features of 3d emission observed in the photoemission experiment on the ZnPC molecule as will be shown lateron.

The valence orbital structure from our ab initio calculations on ZnN_4 is not too much different from results of an Extended Hückel Theory (EHT) study on ZnPC by Schaffer et al. (3). Their population analysis gives a Zn $3d^{9.99}\ 4s^{0.65}\ 4p^{0.91}$ population suggesting a $Zn^{+0.45}$ in ZnPC compared to our result ($Zn^{+0.73}$ in ZnN_4). The slightly increased positive charge on the metal atom in our model could be explained by the missing influence of the peripheral PC part but can also be due to the uncertainty of the population analysis used in the two studies. The valence level diagrams given in Ref. (3) indicate that the energetically highest occupied orbitals in ZnPC are mainly characterized by 2p-type contributions from N centers of the peripheral PC part and can therefore not be described in our ZnN_4 model. Unfortunately, Schaffer et al. (3) do not consider the energy levels of the lower lying valence orbitals in particular of the Zn 3d orbitals which are of interest for the present study.

Since the ground state of ZnN_4 is singlet ($^1A_{1g}$), the absolute values of the Hartree-Fock orbital energies given in Fig. 4 are equal to the ionization potentials (IP) of the respective hole states in frozen orbital (Koopmans) approximation. In this approach, the orbitals are not allowed to relax in response to the removal of the ionized electron yielding IP values that are too large compared to the experimental data. In order to account for this relaxation effect, we have computed, for the case of Zn 3d ionization in ZnN_4, self-consistent wavefunctions of the respective final doublet hole states $^2\Phi_{3d}(i)$ where i = $1e_g$, $1b_{2g}$, $6a_{1g}$, $3b_{1g}$. Then the relaxed IP for ionization out of a given 3d orbital i is determined by the difference between the cluster total energies of the self-consistent final state and the ground state

$$IP_R(i) = E_{tot}(ZnN_4^+,\ ^2\phi_{3d}(i)) - E_{tot}(ZnN_4,\ ^1A_1) \qquad (1)$$

The numerical results for $IP_R(i)$ are shown on the right of Figure 4. Clearly, the relaxed IP values are decreased with respect to the Koopmans data by about 6 eV which is reasonable in view of the fact that the Zn 3d orbitals are rather strongly localized on the metal atom in ZnN_4. The relaxation decrease differs slightly for the different d orbital IP's due to variations in the detailed relaxation mechanism. In particular, the relaxation contribution to the d_{xy}-type ($3b_{1g}$) orbital IP is somewhat smaller compared to the others (this can be understood by the fact that the $3b_{1g}$ orbital, being an antibonding mixture of Zn $3d_{xy}$ and N 2p contributions in the initial state, becomes less antibonding in the self-consistent final state). As a result, the energy range of the relaxed Zn 3d IP's ($\Delta E \sim 1.4$ eV) is decreased with respect to the Koopmans value ($\Delta E \approx 2.0$ eV) as can be seen from Figure 4. The relaxed orbital IP's of our model have to be compared with the photoemission data on the ZnPC molecule as will be discussed lateron.

It is interesting to compare our computed results for the 3d-type levels in ZnN_4 with a simple ligand field model (22). The symmetry of the cluster (and of ZnPC) is described by the symmetry group D_{4h}. Thus, the angular momentum expansion of the ligand potential around the central Zn atom

$$V(\underline{r}) = \sum_{\ell} \sum_{m} v_{\ell m}(r)\ Y_{\ell m}(\hat{\underline{r}}) \qquad (2)$$

contains only contributions with $\ell = 0, 2, 4 \ldots$ and $m = 0, 4, 8 \ldots$. It is easy to show that for this geometry the energy levels of the d-type orbitals of the central atom, neglecting spin-orbit coupling, are given by

$$\varepsilon_1 = b(0,0) + b(2,0) + b(4,0) \qquad \text{for } d_{z^2}\ (a_{1g}) \qquad (3)$$

$$\varepsilon_2 = b(0,0) - b(2,0) + \frac{1}{6}\, b(4,0) + b(4,4) \quad \text{for } d_{x^2-y^2} (b_{2g}) \qquad (4)$$

$$\varepsilon_3 = b(0,0) - b(2,0) + \frac{1}{6}\, b(4,0) - b(4,4) \text{ for } d_{xy}\ (b_{1g}) \qquad (5)$$

$$\varepsilon_{4,5} = b(0,0) + \frac{1}{2}\, b(2,0) - \frac{2}{3}\, b(4,0) \quad \text{for } d_{xz},\ d_{yz}\ (e_g) \qquad (6)$$

where $b(\ell, m)$ are appropriate integrals of metal d radial functions and the potential contribution $v_{\ell m}(r)$. The relative positions (i.e. the splitting) of the four levels agree with those of the relaxed d-hole states in ZnN_4 for interaction parameters

$$b(2,0) = -0.54 \text{ eV},\ b(4,0) = 0.62 \text{ eV and } b(4,4) = -0.59 \text{ eV} \qquad (7)$$

which do not seem to be unrealistic in view of the relatively weak Zn-PC bonding.

4. Discussion

First, we consider the observed binding energies of the 3d derived states in ZnPC. As is apparent from Fig. 2 and Table 1 there is a gas to solid shift of roughly 3.2 eV for the 3d binding energies in going from atomic Zn to the solid state. This shift is mainly caused by the relaxation in the final state for metallic Zn. For ZnPC the binding energy of the d derived state of 15.2 eV is intermediate between gas and metal. Here the gas to solid shift is only 2.1 eV which is in accord with the expectation that the 3d hole can be screened only to a lesser extent in the molecular crystal than in metallic Zn leading to a smaller relaxation shift. Our calculations for the ZnN_4 cluster yield a relaxation shift of roughly 6 eV as can be seen from the comparison of the Koopman's values with the relaxed orbital IP's (Fig. 4). This value is still too small by about 2.3 eV to bring the calculated IP's in agreement with the experiment. There are two reasons why this is so: (i) In the cluster calculation the influence of the peripheral parts of the PC molecule on the 3d-derived orbitals has been neglected, and (ii) the additional relaxation in the condensed phase has to be considered. While the value of 15.2 eV is the binding energy for solid ZnPC, the calculation deals with molecular ZnN_4 clusters. It is interesting to note that for the ZnPC valence orbitals a gas to solid shift of roughly 0.5 eV results if we compare our results with gas phase photoelectron spectra (24). Thus, if we consider this additional relaxation, the calculated center of the 3d derived states is shifted closer to the experimental value.

The width of the 3d derived states in ZnPC (1.2 ± 0.1 eV) is considerably larger than the experimentally determined spin orbit splitting in the gas phase (0.33 eV) and it is also markedly larger than the width of the metallic d-bands (1.02 eV) (see Table 1). The calculated spread of the d-derived states for the ZnN_4 cluster is 2.1 eV for the Koopman's values. It shrinks to 1.4 eV in the relaxed case in good agreement with the experimental value of 1.2 eV for ZnPC.

Thus we conclude that both the binding energies and splittings of the Zn 3d derived valence orbitals in ZnPC can be quite accurately described by model calculations for a ZnN_4 cluster. It would be interesting to see whether this close agreement can also be achieved for other 3d metals such as Cu and Ni where the lower 3d binding energies lead to a larger overlap with N 2p derived orbitals in the PC's (8, 9). Calculations along these lines are currently underway.

Finally, a discussion of the core level structure including a study of shake-up satellites, which we have not considered here, would be interesting, since hybridization in the initial state can be neglected.

Acknowledgement

This work has been supported in part by the Bundesministerium für Forschung und Technologie (BMFT) from funds for synchrotron radiation research. The support of the Synchrotron Radiation Center, University of Madison, is gratefully acknowledged. We wish to thank D.E. Eastman, F.-J. Himpsel and T.C. Chiang (IBM Yorktown Heights) for the kind hospitality in their group and for the many stimulating discussions.

REFERENCES

(1) see e.g. S.C. Mathur, J. Singh and B. Kumar, phys. stat. sol. (b) 48, 843 (1971)

(2) A. Henrickson and M. Sundbom, Theoret.chim.Acta (Berl.) 27, 213 (1972)

(3) A.M. Schaffer, M. Gouterman and E.R. Davidson, Theoret.chim.Acta 30,9 (1973)

(4) M.V. Zeller and R.G. Hayes, J.Am.Chem.Soc. 95, 3855 (1973); A.J. Signorelli and R.G. Hayes, J.Chem.Phys. 64, 4517 (1976); and S. Muralidharan and R.G. Hayes, J.Chem.Phys. 71, 2970 (1979)

(5) H. Hoechst, A. Goldmann, S. Hüfner and H. Malter, phys.stat.sol. (b) 76, 559 (1976)

(6) E. E. Koch and W. Grobman, J. Chem. Phys. 67, 837 (1977)

(7) M. Iwan, W. Eberhardt, G. Kalkoffen, E.E. Koch and C. Kunz, Chem. Phys. Letters 62, 344 (1979)

(8) M. Iwan and E.E. Koch, Solid State Communications 31, 261 (1979)

(9) M. Iwan, E. E. Koch, T.C. Chiang, D.E. Eastman and F.J. Himpsel, Solid State Comm. 34, 57 (1980)

(10) M. Iwan, E.E. Koch, T.C. Chiang and F.J. Himpsel, Physics Letters 76A, 177 (1980)

(11) E. Tegeler, M. Iwan and E.E. Koch, J. Electr.Spectr. 1981, in press

(12) S. Süzer, S.T.Lee and D.A. Shirley, Phys. Rev. A13, 1842 (1976)

(13) F.J. Himpsel, D.E. Eastman, E.E. Koch and A.R. Williams, Phys. Rev. B 22, 4604 (1980)

(14) A.B.P. Lever, Advances in Organic Chemistry and Radiochemistry 7, 27 (1965)

(15) M. Fischer, D.H. Templeton, A. Zalkin and M. Calvin, J. Amer. Chem. Soc. 93, 2622 (1971)

(16) B.P. Tonner, Nucl. Instr. Methods 172, 133 (1980)

(17) D.J. Kennedy and S.T. Manson, Phys. Rev. A5, 227 (1972)

(18) L.I. Johansson, I. Lindau, M. Hecht, S.M. Goldberg and C.S. Fadley, Phys. Rev. B20, 4126 (1979)

(19) see e.g.: J. Barth, Phys. Rev. B, in press; J. Barth, R. Bruhn, B. Sonntag and J. Weaver, Phys. Lett. 78A, 331 (1980)

(20) F.B. van Diujneveldt, IBM Research Report No. RJ 945 (1971) (unpublished)

(21) A.J.H. Wachters, J. Chem. Phys. 52, 1033 (1970)

(22) H.L. Schläfer and G. Gliemann, Einführung in die Ligandenfeldtheorie, Akad. Verlagsges., Frankfurt, 1967

(23) F.J. Himpsel, E.E. Koch and D.E. Eastman, Free electron-like bulk and surface states for Zn(0001), submitted to Phys. Rev. B.

(24) J. Berkowitz, J. Chem. Phys. 70, 2819 (1979)

Table 1

Comparison of the experimentally determined binding energies and widths of the s, p and d derived states for atomic Zn (12), Zn Phthalocyanine (ZnPC) and Zn metal (13). The calculated ionization potentials for a ZnN_4 cluster are also given. All energies are in eV. The binding energies are given with respect to the vacuum level (E_{VAC} = 0) taking a work function of e ϕ = 4.4 eV for Zn metal (13).

	Zn atom[a]	ZnN_4[b]	ZnPC[b]	Zn metal[c]
	binding energies (eV)			
$3d^{10}$ 4s $^2S_{1/2}$	9.39		-	s p band extending from 4.4 to $\approx$ 14.7[d]
$3d^{10}$ 4p $^2P_{1/2}$	15.40		-	
$3d^{10}$ 4p $^2P_{3/2}$	15.51		-	
$3d^9$ $4s^2$ $^2D_{5/2}$	17.17	d_{xy} 16.88 $d_{x^2-y^2}$ 17.02	15.2	14.17
$3d^9$ $4s^2$ $^2D_{3/2}$	17.50	d_{z^2} 17.50 $d_{xz, yz}$ 18.28		
	width (FWHM) of d-derived states			
	0.33	1.4	1.2±0.1	1.02

(a) S. Süzer et al., Ref. 12

(b) this work

(c) F.J. Himpsel et al., Ref. 13

(d) F.J. Himpsel et al., Ref. 23

Figure Captions

Figure 1	A family of photoelectron energy distribution curves for Zn-Phthalocyanine in the valence band range for photon energies between 40 and 100 eV. The maximum due to the Zn derived 3d-states is located at a binding energy ~ 15.2 eV below the vacuum level E_{VAC}.
Figure 2	Photoelectron energy distribution curves for Zn-PC (solid line) and H_2-PC (dashed line) are shown at $h\nu$ = 100 eV in the upper part. Counting rates have been set equal at $E_B \approx$ 30 eV where no pronounced valence band structure is observed. The difference spectrum (Zn-PC minus H_2-PC) $\Delta N(E)$ (middle part) is compared to the EDC's of atomic (12) and metallic Zn (13) (lower panel). The binding energy scales of the upper and middle panel and of the atomic spectrum refer to E_{VAC} = 0. For the solid spectrum eΦ = 4.4 eV has been added to E_{Fermi} for this comparison.
Figure 3	Contour plots for the $7a_{1g}$, $5e_{ux}$, $2b_{1g}$ and $3b_{1g}$ orbitals in a ZnN_4 cluster. In the lowest panel the geometry used for the cluster calculations is given.
Figure 4	Results of the cluster calculation for a ZnN_4 cluster. In the left part, the Hartree Fock one-electron energies of the ZnN_4 valence orbitals are shown. For the d-type orbitals the relaxed ionization potentials are shown in the right part.

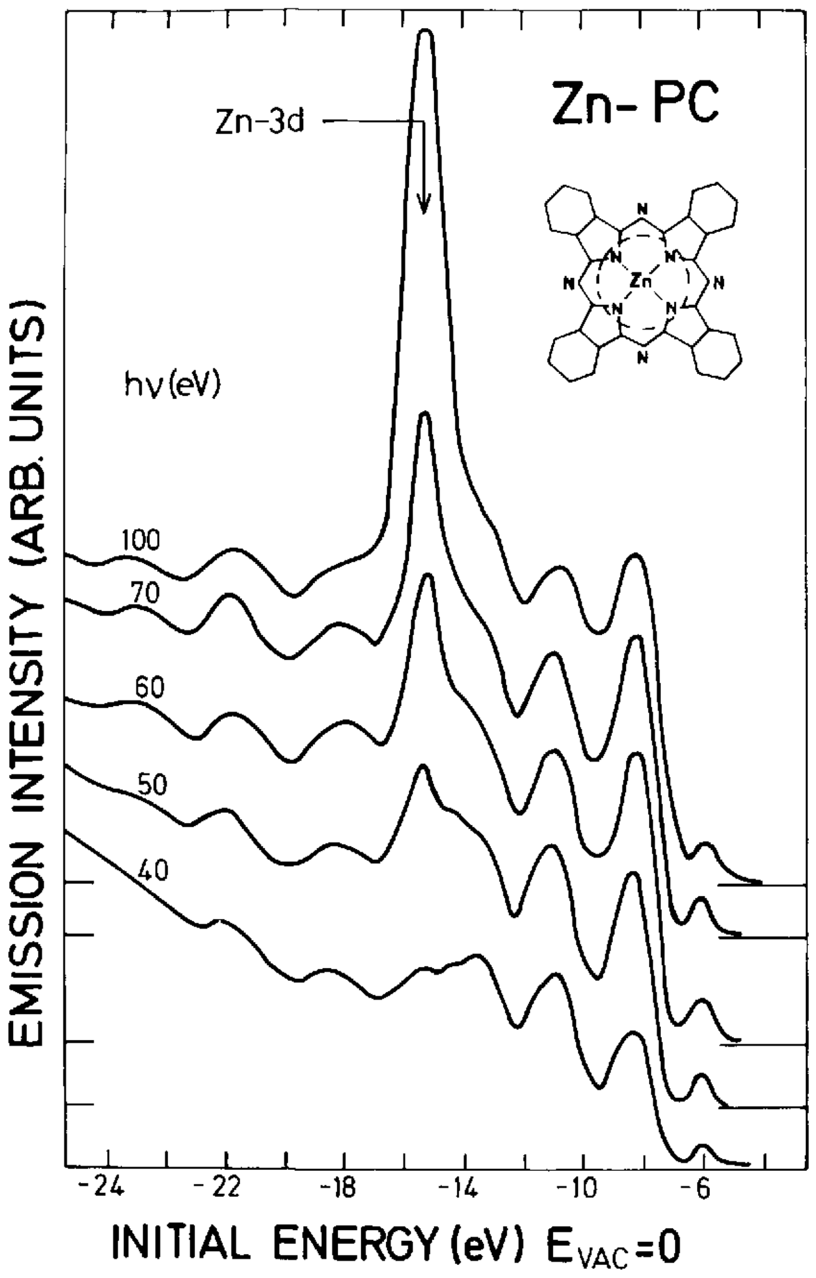
Zn- PC
Zn-3d
N
Zn
hν(eV)
100
70
60
50
40
EMISSION INTENSITY (ARB. UNITS)
-24
-22
-18
-14
-10
-6
INITIAL ENERGY (eV) E_VAC=0

Fig. 1

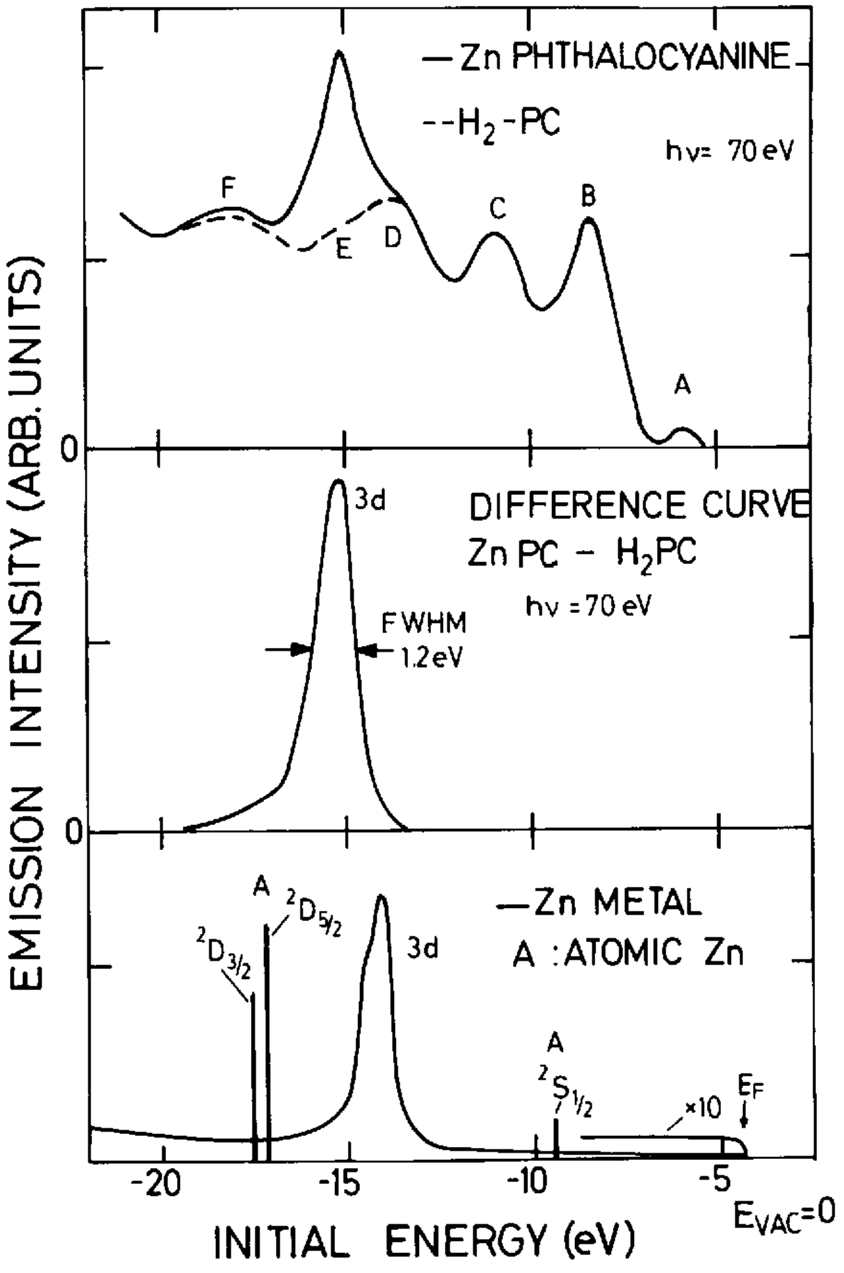
— Zn PHTHALOCYANINE
-- H2-PC
hν= 70 eV
A
B
C
D
E
F
0
3d
DIFFERENCE CURVE
Zn PC − H2PC
hν =70 eV
FWHM
1.2eV
0
— Zn METAL
A : ATOMIC Zn
A
2D5/2
2D3/2
3d
A
2S1/2
×10
EF
EMISSION INTENSITY (ARB. UNITS)
-20
-15
-10
-5
E_VAC=0
INITIAL ENERGY (eV)

Fig. 2

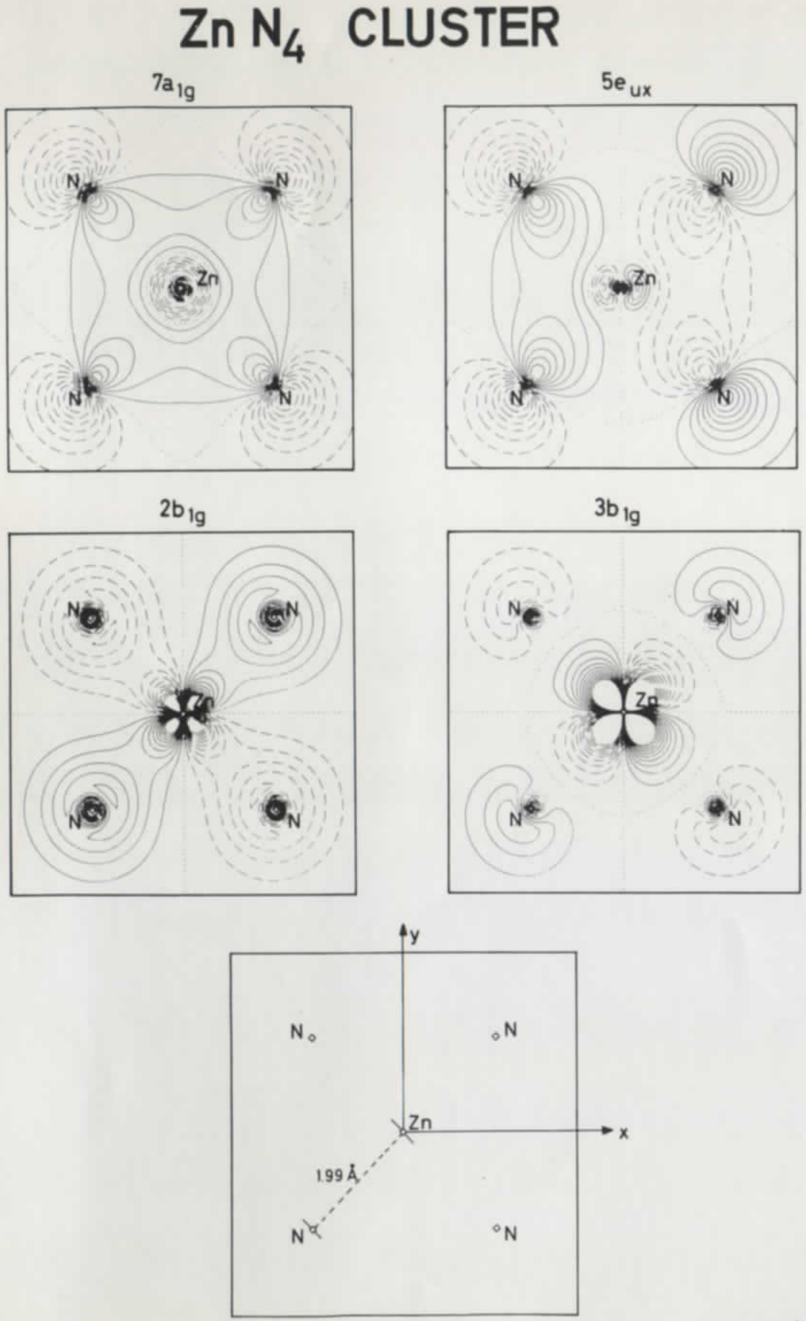
Zn N4 CLUSTER
7a1g
5eux
2b1g
3b1g
N
Zn
y
x
1.99 Å

Fig. 3

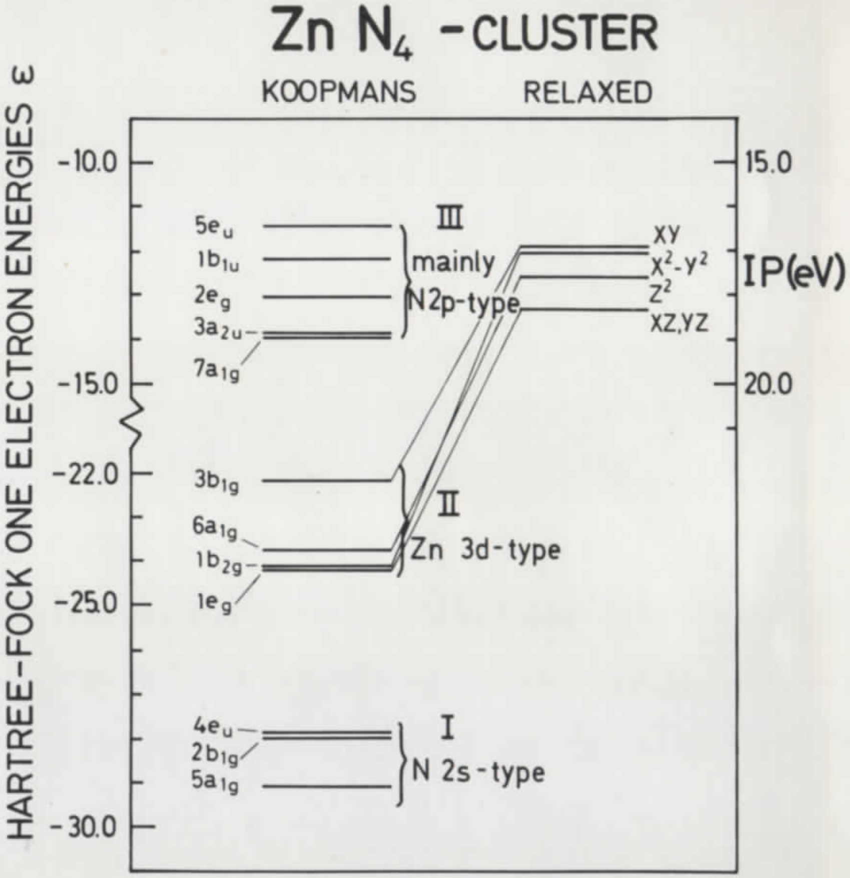
Zn N4 -CLUSTER
KOOPMANS
RELAXED
HARTREE-FOCK ONE ELECTRON ENERGIES ε
-10.0
-15.0
-22.0
-25.0
-30.0
15.0
20.0
IP(eV)
5eu
1b1u
2eg
3a2u
7a1g
III
mainly
N2p-type
xy
x²-y²
z²
xz,yz
3b1g
6a1g
1b2g
1eg
II
Zn 3d-type
4eu
2b1g
5a1g
I
N 2s-type

Fig. 4